Enhancing Kondo coupling in alkaline-earth-metal atomic gases with confinement-induced resonances in mixed dimensions

Yanting Cheng,[1] Ren Zhang,[1,*] Peng Zhang,[2,3,†] and Hui Zhai[1,4]
[1]*Institute for Advanced Study, Tsinghua University, Beijing, 100084, China*
[2]*Department of Physics, Renmin University of China, Beijing, 100872, China*
[3]*Beijing Computational Science Research Center, Beijing, 100084, China*
[4]*Collaborative Innovation Center of Quantum Matter, Beijing, 100084, China*
(Received 14 September 2017; published 4 December 2017)

The Kondo effect describes the spin-exchange interaction between localized impurities and itinerant fermions. The ultracold alkaline-earth atomic gas provides a natural platform for quantum simulation of the Kondo model, utilizing its long-lived clock state and the nuclear-spin exchange interaction between clock state and ground state. One of the key issue now is whether the Kondo temperature can be high enough to be reached in current experiments, for which we have proposed to use transverse confinement to confine atoms into a one-dimensional tube and to use the confinement-induced resonance to enhance Kondo coupling. In this work, we further consider the $(1+0)$-dimensional scattering problem when the clock state is further confined by an axial harmonic confinement. We show that this axial confinement for the clock-state atoms not only plays a role for localizing them, but can also act as an additional control knob to reach the confinement-induced resonance. We show that, in the presence of both the transverse and the axial confinements, the confinement-induced resonance can be reached in the practical conditions and the Kondo effect can be attainable in this system.

DOI: 10.1103/PhysRevA.96.063605

I. MOTIVATION AND BACKGROUND

In the past decades, experiments in cold-atom systems have successfully explored many intriguing quantum many-body phenomena of different paradigms, including fermion pairing and the BCS-BEC crossover, the Bose and the Fermi Hubbard models [1], the Kosterlize–Thouless transition [1], one-dimensional integrable models [2], and spin-orbit coupling [3] and topological models [4]. Exploring these phenomena with cold atom systems has a list of advantages; for instance, one can access physical quantities that have not been measured before in their condensed-matter realizations, and one can also study nonequilibrium dynamics in a highly controllable way. However, until now there is still one important category that has yet to be experimentally realized with cold-atom systems, despite quite a few existing proposals [5–14]; that is, Kondo physics.

The Kondo model describes the spin-exchange interaction between localized impurities and itinerant fermions [15]. The alkaline-earth atomic gases have natural advantages for performing quantum simulations of the Kondo model. The schematic energy level of single alkaline-earth atoms is shown in Fig. 1. First of all, there is a long-lived electronic excited state known as the clock state, and usually denoted by $|e\rangle$. Atoms in this clock state generically have a different ac polarizability compared with atoms in their electronic ground state, which is usually denoted by $|g\rangle$, except for lasers with a magic wavelength [16,17]. Therefore, it is easy to realize a situation in which lasers create a deep lattice for $|e\rangle$ atoms and make them localized as impurities, while $|g\rangle$ atoms experience quite a shallow lattice and remain itinerant, as shown in Fig. 2(a).

Second, in addition to the orbital degree of freedom symbolized by $|g\rangle$ and $|e\rangle$, there is also a nuclear-spin degree of freedom. Due to the nearly perfect decoupling between the nuclear spin and the electronic degree of freedoms in these two states of alkaline-earth atoms [18], the interaction has to be invariant under nuclear-spin rotation. Thus, the interaction has to be diagonal in the nuclear-spin singlet and three triplet channels, and for the s-wave interaction subjected to the symmetrization condition of the entire wave function, these channels also have to be orbital triplet and singlet, respectively. Considering the interaction between one atom in the $|g\rangle$ state and one atom in the $|e\rangle$ state, we have the following relevant basis [19,20]:

$$|+\rangle = \tfrac{1}{2}(|ge\rangle + |eg\rangle)(|\uparrow\downarrow\rangle - |\downarrow\uparrow\rangle), \tag{1}$$

$$|-,0\rangle = \tfrac{1}{2}(|ge\rangle - |eg\rangle)(|\uparrow\downarrow\rangle + |\downarrow\uparrow\rangle), \tag{2}$$

$$|-,1\rangle = \tfrac{1}{\sqrt{2}}(|ge\rangle - |eg\rangle)|\uparrow\uparrow\rangle, \tag{3}$$

$$|-,-1\rangle = \tfrac{1}{\sqrt{2}}(|ge\rangle - |eg\rangle)|\downarrow\downarrow\rangle, \tag{4}$$

where $+$ and $-$ denote orbital triplet and singlet, respectively, and in $|-,q\rangle$, q denotes the total nuclear spin along the $\hat{z}$ direction.

In three dimensions, the two-body interaction can be written as

$$V(\mathbf{r}) = V_+(\mathbf{r})|+\rangle\langle+| + \sum_{q=0,\pm1} V_-(\mathbf{r})|-,q\rangle\langle-,q|, \tag{5}$$

where $\mathbf{r}$ is the relative coordinate between a $|g\rangle$ and an $|e\rangle$ atom. V_+ and V_- are both short-ranged potentials, and they are featured by two scattering lengthes of $a_{s,+}$ and $a_{s,-}$,

*rine.zhang@gmail.com
†pengzhang@ruc.edu.cn

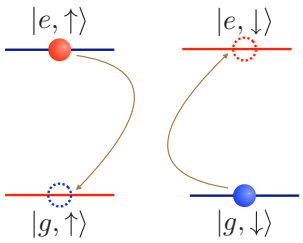

FIG. 1. Schematic energy levels for alkaline-earth atoms. The red ball and red dashed circle represent the $|e\rangle$ atom (long-lived clock state). The blue ball and blue dashed circle represent the $|g\rangle$ atom (ground state). Nuclear-spin exchange happens when the $|e\rangle$ atom and $|g\rangle$ atom collide.

respectively. Expanding $V(\mathbf{r})$ into the basis of

$$|g\uparrow;e\downarrow\rangle = \tfrac{1}{\sqrt{2}}(|+\rangle + |-,0\rangle), \tag{6}$$

$$|g\downarrow;e\uparrow\rangle = \tfrac{1}{\sqrt{2}}(|-,0\rangle - |+\rangle), \tag{7}$$

and $|-,\pm 1\rangle$, we can reconstruct the interaction as

$$\begin{aligned} V(\mathbf{r}) = {} & \frac{V_+(\mathbf{r})+V_-(\mathbf{r})}{2}(|g\uparrow;e\downarrow\rangle\langle g\uparrow;e\downarrow| \\ & + |g\downarrow;e\uparrow\rangle\langle g\downarrow;e\uparrow|) \\ & + \frac{V_-(\mathbf{r})-V_+(\mathbf{r})}{2}(|g\uparrow;e\downarrow\rangle\langle g\downarrow;e\uparrow| \\ & + |g\downarrow;e\uparrow\rangle\langle g\uparrow;e\downarrow|) \\ & + V_-(\mathbf{r})|-,1\rangle\langle -,1| + V_-(\mathbf{r})|-,-1\rangle\langle -,-1|. \end{aligned} \tag{8}$$

Here one can see that the key point is that the difference of between V_+ and V_- gives rise to a spin-exchanging interaction between $|g\rangle$ and $|e\rangle$ atoms, as shown in Fig. 2(b), whose effect is most profound in the zero-field limit where the single-particle energies of $|g\uparrow;e\downarrow\rangle$ and $|g\downarrow;e\uparrow\rangle$ are degenerate. Actually, such spin-exchange processes have been observed in experiments [19,20]. This magnetic-field regime, when $|g\rangle$ atoms are itinerant and $|e\rangle$ atoms are localized, will give rise to a Kondo model.

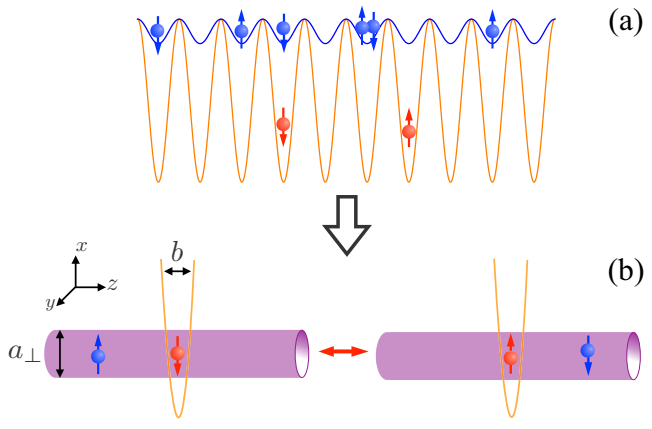

FIG. 2. (a) A pair of laser beams creates a deep lattice for atoms in the clock state $|e\rangle$ and a weak lattice for atoms in the ground state $|g\rangle$. (b) The key process responsible for the Kondo effect is the spin-exchange scattering between impurity (localized $|e\rangle$ atom) and the itinerant fermions ($|g\rangle$ atoms). The blue and red balls denote the ground state and the clock state, respectively. The nuclear spins are denoted by arrows.

It looks like everything is ready. However, there is a last challenge to overcome. That is, since in cold-atom systems it is hard to achieve a temperature regime that is orders of magnitude lower than the Fermi temperature, it is important to increase the strength of the spin-exchange interaction such that the Kondo temperature becomes high enough to be attainable by current cooling capabilities.

To solve this problem, in the previous work, we propose a scheme to use confinement-induced resonance to increase the Kondo coupling [13]. The basic idea is to use lasers with magic wavelength to create a two-dimensional lattice, with which atoms in both the $|g\rangle$ and $|e\rangle$ state are confined into a one-dimensional tube with the same transverse confinement radius $a_\perp$. With the standard formula of the confinement-induced resonance [21], at zero field the reduced interaction in one dimension still takes the form of Eq. (5), with $V_\xi = g_\xi\delta(z)$ ($\xi = +,-$), and

$$g_\xi = \frac{4\hbar^2 a_{s,\xi}}{m a_\perp^2}\left(1 - \mathcal{C}\frac{a_{s,\xi}}{a_\perp}\right)^{-1}, \quad \mathcal{C} \approx 1.460\,35\ldots. \tag{9}$$

Thus, when $a_\perp$ approaches either $\mathcal{C}a_{s,+}$ or $\mathcal{C}a_{s,-}$, one of the g_ξ will diverge while the other remains finite. Hence, their difference will become very large and the Kondo effect will be enhanced. In Ref. [13] we have also considered the correction due to a finite Zeeman field, and we find that the effect is insignificant in the low-field regime. Thus, in this paper we only consider the zero-field case for simplicity.

Nevertheless, it still does not complete the whole story for two reasons: First, on the experimental side, to enforce the system to be in the one-dimensional regime, $a_\perp$ should be sufficiently small; on the other hand, due to the practical constraint of the laser power, $a_\perp$ also cannot be arbitrarily small. That is, there is a range over which $a_\perp$ can be tuned and, within this range, $a_\perp$ may reach neither $\mathcal{C}a_{s,+}$ nor $\mathcal{C}a_{s,-}$. Second, on the theory side, in Ref. [13] the axial confinement for the localized $|e\rangle$ atoms is only treated at the level of the lowest Wannier wave function approximation. Such an approximation may fail in certain parameter regimes.

Motivated by the experimental efforts along this direction [22], the present work treats a $(1+0)$-dimensional scattering problem that solves these two problems simultaneously. Here we treat the axial confinement for $|e\rangle$ atoms beyond the Wannier wave function approximation and will show that it indeed gives rise to much richer features. In particular, we show that this axial confinement length b [as shown in Fig. 2(b)] plays a role as an extra control parameter to reach confinement-induced resonance. That is, even if $a_\perp$ is not very close to $\mathcal{C}a_{s,+}$ or $\mathcal{C}a_{s,-}$, one can still reach resonance by tuning b with the axial confinement.

II. MODEL

To be numerically tractable, we simplify the problem from the lattice case as shown in Fig. 2(a) to a $(1+0)$-dimensional problem, as shown in Fig. 2(b). This simplification includes following assumptions: (i) For $|e\rangle$ atoms, we assume that it

is always localized in one of the lattice sites, and we expand the potential to the quadratic order nearby its minimum. That is, we ignore the anharmonic part of the lattice potential. The axial-confinement problem is treated as a harmonic trap with frequency ω_z. (ii) The laser beam still induces a weak lattice potential for the $|g\rangle$ atom, although the ac polarizabilities of the $|g\rangle$ state and $|e\rangle$ state can differ a lot. Here we take this effect into account by an effective mass approximation; that is, we still assume single-particle dispersion for $|g\rangle$ atom is a parabola but with an effective mass denoted by m_g. In general $m_g > m$ (m is the bare mass). Since in one dimension the density of state diverges at zero energy and the low-energy states contribute most to the scattering problem [23], we believe that the effective-mass approximation is reasonably good in one dimension.

We will show that, even with these two approximations, the results should be qualitatively good, and the results can be systematically improved later by including the anharmonicity for the localized atoms and other lattice effects for the itinerant atoms. Furthermore, in principle, we should solve the problem in three dimensions by including the transverse confinement for both states and the axial confinement solely for $|e\rangle$ atoms on the equal footing. However, here we simplify the procedure by first treating the transverse confinement with Eq. (9), and subsequently studying the $(1+0)$ dimension. We believe this treatment is sufficiently good because the resonances induced by transverse confinement and the axial confinement are two different physical processes and they generally will not strongly interfere with each other.

We now start with the one-dimensional Hamiltonian of the form

$$\hat{H}_{\rm tot} = \hat{H}_+|+\rangle\langle +| + \sum_{q=0,\pm 1} \hat{H}_-|-,q\rangle\langle -,q|. \tag{10}$$

Here

$$\hat{H}_\xi = -\frac{\hbar^2}{2m_g}\frac{d^2}{dz_g^2} - \frac{\hbar^2}{2m}\frac{d^2}{dz_e^2} + \frac{1}{2}m\omega_z^2 z_e^2 + g_\xi \delta(z_e - z_g) \tag{11}$$

for $\xi = +,-$, with z_g and z_e being the positions of the $|g\rangle$ state and $|e\rangle$ state, respectively.

III. METHOD

Previously, scattering problems in mixed dimensions such as $3+0$, $3+1$, or $3+2$ were studied theoretically [24–27] and experimentally [28]. Here the problem we considered a $(1+0)$-dimensional. Since the Hamiltonian is diagonal in the basis chosen in Eq. (10), we only need to solve the Hamiltonian (11), and the difference in the effective interaction strength between the $|+\rangle$ and $|-,0\rangle$ channels gives rise to the spin-exchange strength.

Because of the additional harmonic trap along the axial direction for the $|e\rangle$ atom, the relative motion of the $|g\rangle$ atom and $|e\rangle$ atom is not separable from their center-of-mass motion. Here we consider the scattering between a moving $|g\rangle$ atom with momentum $\hbar k$ ($k > 0$) along the z direction and an $|e\rangle$ atom in the ground state of the trap. The incident wave function is given by

$$\psi_k^0(z_g,z_e) = \frac{1}{\sqrt{2\pi}} e^{ikz_g}\phi_0(z_e), \tag{12}$$

where $\phi_0(z_e) = \exp(-z_e^2/2b^2)/(\pi^{1/4}b^{1/2})$ is the ground-state wave function of the harmonic trap. $b = \sqrt{\hbar/m\omega_z}$ is the harmonic trap length for the axial trap. For our system the two-body scattering wave function $\psi_k^+(z_g,z_e)$ is given by the Lippmann–Schwinger equation

$$\psi_k^+(z_g,z_e) = \psi_k^0(z_g,z_e) + g_\xi \int dz' G_0(z_g,z_e;z',z')\psi_k^+(z',z'). \tag{13}$$

Here, $G_0(z_g,z_e;z_g',z_e')$ is the two-body free Green's function. In this paper we consider the low-energy scattering process where $\hbar^2k^2/(2m_g) < \hbar\omega_z$. For this case we have

$$\begin{aligned} G_0(z_g,z_e;z_g',z_e') = &-i\frac{m_g}{\hbar^2}\frac{e^{ik|z_g-z_g'|}}{k}\phi_0(z_e)\phi_0^*(z_e') \\ &-\frac{m_g}{\hbar^2}\sum_{n=1}^{\infty}\frac{e^{-\sqrt{2m_gn\omega_z/\hbar^2-k^2}|z_g-z_g'|}}{\sqrt{2m_gn\omega_z/\hbar^2-k^2}} \\ &\times\phi_n(z_e)\phi_n^*(z_e'), \end{aligned} \tag{14}$$

with $\phi_n(z) = (b\sqrt{\pi}2^n n!)^{-1/2}\exp(-z^2/2b^2)H_n(z/b)$ ($n = 1,2,\ldots$) being the nth eigen wave function of the harmonic trap.

Equations (13) and (14) imply that, in the limit of $|z_g| \to \infty$, the scattering wave function $\psi_k^+(z_g,z_e)$ can be expressed as

$$\begin{aligned} \psi_k^+(|z_g|\to\infty,z_e) = \frac{1}{\sqrt{2\pi}}\big[&e^{ikz_g} + f_\xi^{\rm even}(k)e^{ik|z_g|} \\ &+ f_\xi^{\rm odd}(k)\,{\rm sign}(z_g)e^{ik|z_g|}\big]\phi_0(z_e). \end{aligned} \tag{15}$$

Here $f_\xi^{\rm even}(k)$ and $f_\xi^{\rm odd}(k)$ are the effective one-dimensional (1D) scattering amplitudes for the even and odd partial waves, respectively, and are given by

$$f_\xi^\ell(k) = -i\sqrt{2\pi}\frac{m_g}{\hbar^2}\frac{g_\xi}{k}\int dz' F_\ell(kz')\phi_0^*(z')\psi_k^+(z',z'), \tag{16}$$

for $\ell = $ (even, odd), respectively, with $F_{\rm even}(kz') = \cos(kz')$ and $F_{\rm odd}(z') = -i\sin(kz')$. Here the function $\psi_k^+(z',z')$ satisfies the integral equation

$$\begin{aligned} \psi_k^+(z',z') = &\psi_k^0(z',z') \\ &+ g_\xi\int dz'' G_0(z',z';z'',z'')\psi_k^+(z'',z''), \end{aligned} \tag{17}$$

which is a straightforward result of Eq. (13).

In this paper we focus on the low-energy limit of $k \to 0$. In this limit the scattering amplitude for the odd partial wave is negligible and the scattering of the even partial wave is described by the effective one-dimensional scattering length $a_\xi^{\rm eff}$, which is defined as

$$a_\xi^{\rm eff} = \lim_{k\to 0}\frac{i}{k}\left[1 + \frac{1}{f_\xi^{\rm even}(k)}\right]. \tag{18}$$

Explicitly, for $k \to 0$ we have

$$f_\xi^{\text{even}}(k) \approx -\frac{1}{1+ika_\xi^{\text{eff}}}, \quad f_\xi^{\text{odd}}(k) \approx 0. \tag{19}$$

This scattering amplitude can be reproduced by an effective one-dimensional delta potential

$$g_\xi^{\text{eff}}\delta(z_g) \equiv -\frac{\hbar^2}{m_g a_\xi^{\text{eff}}}\delta(z_g). \tag{20}$$

Thus, at low energy the itinerant $|g\rangle$ atoms experience an effective potential $g_\xi^{\text{eff}}\delta(z_g)$. Hence, the place where g_ξ^{eff} diverges (i.e., $a_\xi^{\text{eff}} = 0$) is the location of the scattering resonance in the channel ξ.

By scale $z_g \to z_g/b$, $k \to kb$, and $\phi \to \phi\sqrt{b}$, one can show that Eqs. (13), (16), and (17) become dimensionless, in which the only parameters are the mass ratio m_g/m and the dimensionless interaction strength $\tilde{g}_\xi$ defined as

$$\tilde{g}_\xi \equiv \frac{g_\xi m b}{\hbar^2}. \tag{21}$$

The strength of effective potential g_ξ^{eff} also becomes dimensionless, which is defined as

$$\tilde{g}_\xi^{\text{eff}} \equiv \frac{g_\xi^{\text{eff}} m_g b}{\hbar^2} = -\frac{b}{a_\xi^{\text{eff}}}. \tag{22}$$

$\tilde{g}_\xi^{\text{eff}}$ and a_ξ^{eff} are universal functions of m_g/m and $\tilde{g}_\xi$.

In our calculation, we first numerically solve Eq. (17) to derive the function $\psi_k^+(z',z')$. Substituting the solution into Eqs. (16) and (18), we obtain the one-dimensional scattering length a_ξ^{eff}. By using this result and Eqs. (20)–(22) we finally obtain the universal relation between $\tilde{g}_\xi^{\text{eff}}$ and $\tilde{g}_\xi$, m_g/m.

IV. RESULTS AND ANALYSIS

In Fig. 3 we show $\tilde{g}_\xi^{\text{eff}}$ as a universal function of $\tilde{g}_\xi$, for the mass ratio $m_g/m = 1$ and $m_g/m = 2$, respectively. Here we can see multiple resonances, and the nth of them occurs at $\tilde{g}_\xi = \alpha_n$. For instance, for $m_g/m = 1$ we have $\alpha_1 = 1.71, \alpha_2 = -2.07, \alpha_3 = -3.49, \ldots$, while for $m_g/m = 2$, we have $\alpha_1 = 0.73, \alpha_2 = -1.36, \alpha_3 = -2.62, \ldots$. Similar phenomenon has been obtained in other mixed-dimension systems [24,25].

The occurrence of a series of resonances with negative $\tilde{g}_\xi$ can be understood as follows: Our problem is essentially an infinite-channel scattering problem, and the nth channel corresponds to the $|e\rangle$ atom being in the nth eigenstate of the axial harmonic trap. The threshold energy for the nth channel is $n\hbar\omega_z$ (here we have ignored the zero-point energy of the harmonic trap). Thus, when the kinetic energy of the incoming particle $\hbar^2k^2/(2m_g) < \hbar\omega_z$, only the zeroth channel is open, and all the other channels are closed. For $\tilde{g}_\xi < 0$, this interaction potential can support one bound state in each closed channel. When the energy of this bound state matches the threshold of the open channel, a resonance occurs. Therefore, each closed channel will give rise to one resonance in the negative $\tilde{g}_\xi$ side. The higher the resonance, the less the wave functions overlap and, consequently, the narrower the resonance width.

Note that the effective spin exchanging interaction is proportional to the difference between g_+^{eff} and g_-^{eff}, as shown in Eq. (8). Thus, the place where one of the g_ξ^{eff} ($\xi = \pm$) diverges [i.e., the place where $\tilde{g}_\xi = \alpha_n$ ($n = 1,2,3,\ldots$)] locates a spin-exchange scattering resonance. Combining Eqs. (9) and (21), one can express $\tilde{g}_\xi$ in term of two physical tunable parameters $a_{s,\xi}/a_\perp$ and $b/a_\perp$ as

$$\tilde{g}_\xi = \frac{4a_{s,\xi}b}{a_\perp^2}\left(1 - \mathcal{C}\frac{a_{s,\xi}}{a_\perp}\right)^{-1}, \tag{23}$$

and the resonance position in the $a_{s,\xi}/b - a_{s,\xi}/a_\perp$ plane is determined by the following identity:

$$\frac{4\left(\frac{a_{s,\xi}}{a_\perp}\right)^2}{\frac{a_{s,\xi}}{b}\left(1 - \mathcal{C}\frac{a_{s,\xi}}{a_\perp}\right)} = \alpha_n, \quad n = 1,2,3\ldots. \tag{24}$$

In Fig. 4(a) we show the resonance positions given by Eq. (24) as physical parameters $a_{s,\xi}/b$ and $a_{s,\xi}/a_\perp$ for $m_g = m$. We notice that, in the limit $a_{s,\xi}/b \to \infty$, all the resonance positions will converge to $a_\perp/a_{s,\xi} = \mathcal{C}$. That is because, in this limit, the energy difference of the harmonic oscillator is much larger than the kinetic energy, so that the lowest Wannier wave function approximation in Ref. [13] is valid, and the resonance is precisely where $\tilde{g}_\xi$ diverges.

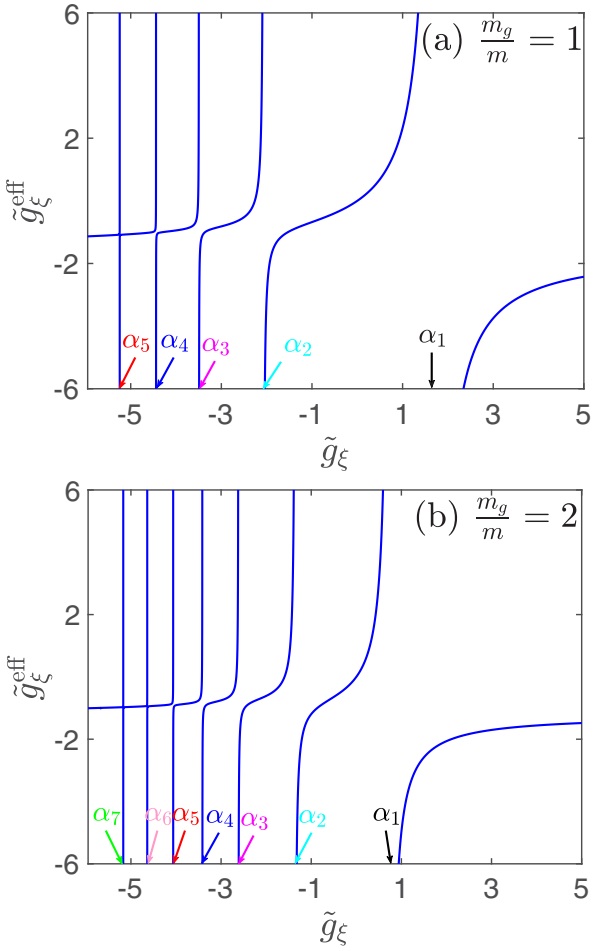

FIG. 3. The dimensionless strength for the effective potential $\tilde{g}_\xi^{\text{eff}}$ as a universal function of the dimensionless bare interaction strength $\tilde{g}_\xi$ with (a) $m_g/m = 1$ and (b) $m_g/m = 2$.

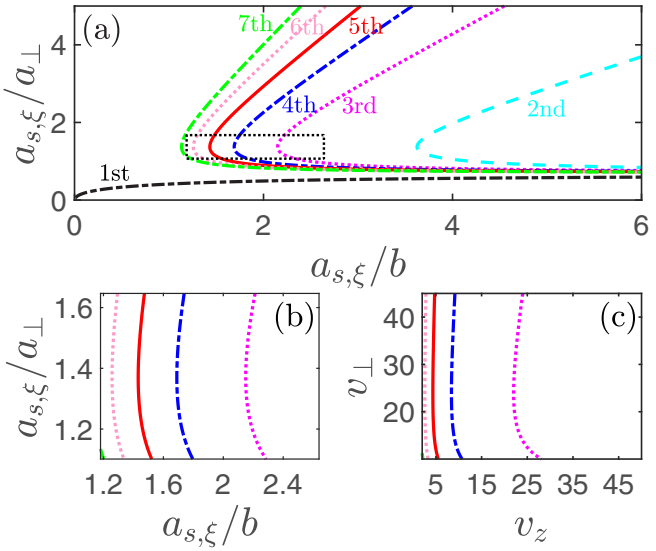

FIG. 4. (a) The position for resonant spin-exchange interaction in the $a_{s,\xi}/a_\perp - a_{s,\xi}/b$ plane for $m_g = m$. The black dotted rectangle indicates the regime that can be attainable with a set of typical parameters for ^{173}Yb atoms. (b) Zoom-in plot of panel (a) for the regime inside the black dotted rectangle. (c) The same plot as in panel (b) with the axes $a_{s,\xi}/a_\perp$ and $a_{s,\xi}/b$ converted into the optical lattice depth $v_\perp$ and v_z, respectively, when the confinement is provided by optical lattice potentials. $v_\perp$ is the transverse lattice depth for both $|g\rangle$ and $|e\rangle$ atoms, and v_z is the axial lattice depth for $|e\rangle$ atoms. In panel (c), we choose $\xi = +$ and $a_{s,+} = 2000a_0$ with a_0 being the Bohr radius.

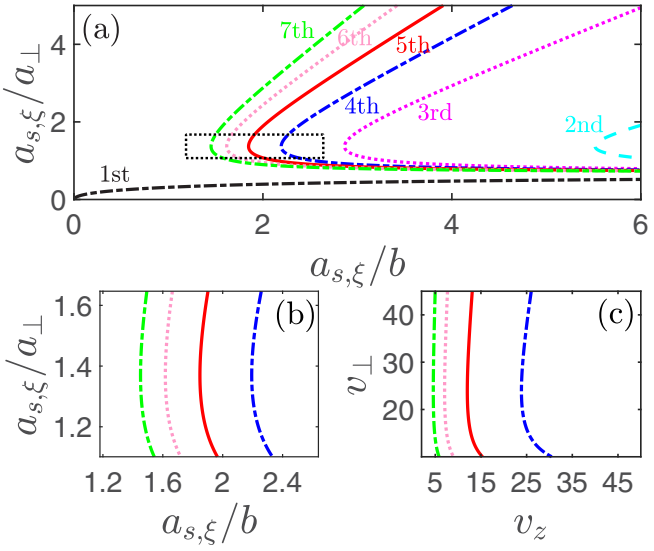

FIG. 5. The same plot as Fig. 4 except for $m_g = 2m$. We plot the resonances up to the seventh one, and other more narrower ones are not shown.

In practice, the confinements are provided by an optical lattice. Considering an optical lattice of the form $v_\perp E_R^\perp[\cos^2(k_{\perp,0}x) + \cos^2(k_{\perp,0}y)]$ for both states, with $E_R^\perp = \hbar^2 k_{\perp,0}^2/(2m)$, and an optical lattice of the form $v_z E_R^z \cos^2(k_{z,0}z)$ for the $|e\rangle$ state, with $E_R^z = \hbar^2 k_{z,0}^2/(2m)$, we have $a_\perp = \lambda_\perp/(\sqrt{2}\pi v_\perp^{1/4})$ and $b = \lambda_z/(2\pi v_z^{1/4})$, where $\lambda_\perp = 2\pi/k_{\perp,0}$ and $\lambda_z = 2\pi/k_{z,0}$. Taking the ^{173}Yb atom as an example, we have $a_{s,+} \approx 2000a_0$, and we use the magic-wavelength laser with $\lambda_\perp = 759$ nm for the transverse confinement, and for the axial lattice we choose the laser with wavelength $\lambda_z = 670$ nm where the ac polarizabilities of both states differ a lot.

With the parameters shown above, the ranges of $a_{s,+}/a_\perp$ and $a_{s,+}/b$ that can be reached with the tunability of lattice depth are indicated by the black dotted rectangle in Fig. 4(a), where one can see that several resonances fall into the rectangle. The zoom-in plot inside the box is shown in Fig. 4(b). Then, with these parameters, we can convert $a_{s,+}/a_\perp$ and $a_{s,+}/b$ into $v_\perp$ and v_z. The resonance locations as a function of $v_\perp$ and v_z is shown in Fig. 4(c).

Figure 5 shows the same plot as Fig. 4, except for the mass ratio is $m_g = 2m$. This is a typical effective mass for a lattice depth of about $5E_R$. One can see that more higher resonances move into the box. Here we only show up to the seventh resonance, because the higher one will get narrower and narrower. Nevertheless, we should also remark that, although these resonances are already quite narrow in the $a_{s,+}/a_\perp - a_{s,+}/b$ plot, they can be reasonably wide in the $v_\perp$-v_z plot because $a_\perp$ and b are not quite sensitive to $v_\perp$ and v_z.

V. SUMMARY AND OUTLOOK

In summary, we have considered a scattering problem for alkaline-earth atoms in a $(1+0)$-dimensional geometry where the ground-state atom is mobile along the tube, while the clock-state atom is confined by an axial harmonic trap, with both atoms subjected to a transverse confinement. We have shown that, in the presence of both proper transverse and axial confinements, the confinement-induced resonance can be reached in ^{173}Yb atoms with practical parameters, where the nuclear-spin exchange interaction can be enhanced significantly. This will lead to a Kondo effect at relatively higher temperature that can be reached in current experiments. Further work along this line will discuss how to detect the Kondo effect in this system and how to utilize this system to enrich our physical understanding of the Kondo effect.

It is also pointed out that our calculation is done for a pure $(1+0)$-dimensional model. In the realistic experiments, the atoms are trapped in a "quasi $(1+0)$-dimensional" system with a strong harmonic transverse confinement in the x-y plane. Nevertheless, in many current experiments the frequency $\omega_\perp$ of the transverse confinement is much larger than Fermi energy E_F of the ultracold gas. For instance, in the experiment of Ref. [29] the transverse frequency is about $\omega_\perp \sim 2\pi \times 80$ kHz, while the typical Fermi energy E_F of an ultracold gas in quasi-1D could be of the order of 2π kHz. For these systems the atoms are almost frozen in the transverse ground state, and thus the main characters of the spin-exchange process (e.g., the appearance of the resonance induced by the longitudinal trapping potential of the $|e\rangle$ atom, as shown in Fig. 3) is dominated by the physics of our $(1+0)$-dimensional model. On the other hand, to further improve the quantitative accuracy of the current results, we need to take in account the contributions from the transverse excited states. This will be done in future works.

ACKNOWLEDGMENTS

We acknowledge Simon Fölling for stimulating discussion. This work was supported by NSFC Grants No. 11325418 (H.Z.), No. 11434011 (P.Z.), and No. 11674393 (P.Z.) and by Tsinghua University Initiative Scientific Research Program (H.Z.), NKBRSF of China under Grant No. 2016YFA0301600 (H.Z.), as well as the Research Funds of Renmin University of China under Grant No. 16XNLQ03 (P.Z.).

[1] I. Bloch, J. Dalibard, and W. Zwerger, Rev. Mod. Phys. **80**, 885 (2008).
[2] X.-W. Guan, M. T. Batchelor, and C. Lee, Rev. Mod. Phys. **85**, 1633 (2013).
[3] H. Zhai, Rep. Prog. Phys. **78**, 026001 (2015).
[4] N. Goldman, J. C. Budich, and P. Zoller, Nat. Phys. **12**, 639 (2016).
[5] G. M. Falco, R. A. Duine, and H. T. C. Stoof, Phys. Rev. Lett. **92**, 140402 (2004).
[6] L.-M. Duan, Europhys. Lett. **67**, 721 (2004).
[7] A. V. Gorshkov, M. Hermele, V. Gurarie, C. Xu, P. S. Julienne, J. Ye, P. Zoller, E. Demler, M. D. Lukin, and A. M. Rey, Nat. Phys. **6**, 289 (2010).
[8] A. Carmi, Y. Oreg, and M. Berkooz, Phys. Rev. Lett. **106**, 106401 (2011).
[9] J. Bauer, C. Salomon, and E. Demler, Phys. Rev. Lett. **111**, 215304 (2013).
[10] Y. Nishida, Phys. Rev. Lett. **111**, 135301 (2013); Phys. Rev. A **93**, 011606 (2016).
[11] M. Nakagawa and N. Kawakami, Phys. Rev. Lett. **115**, 165303 (2015).
[12] L. Isaev and A. M. Rey, Phys. Rev. Lett. **115**, 165302 (2015).
[13] R. Zhang, D. Zhang, Y. Cheng, W. Chen, P. Zhang, and H. Zhai, Phys. Rev. A **93**, 043601 (2016).
[14] I. Kuzmenko, T. Kuzmenko, Y. Avishai, and K. Kikoin, Phys. Rev. B **91**, 165131 (2015).
[15] A. C. Hewson, *The Kondo Problem to Heavy Fermions* (Cambridge University Press, Cambridge, 1993).
[16] Z. W. Barber, J. E. Stalnaker, N. D. Lemke, N. Poli, C. W. Oates, T. M. Fortier, S. A. Diddams, L. Hollberg, C. W. Hoyt, A. V. Taichenachev, and V. I. Yudin, Phys. Rev. Lett. **100**, 103002 (2008).
[17] V. A. Dzuba and A. Derevianko, J. Phys. B: At., Mol. Opt. Phys. **43**, 074011 (2010).
[18] M. M. Boyd, T. Zelevinsky, A. D. Ludlow, S. Blatt, T. Zanon-Willette, S. M. Foreman, and J. Ye, Phys. Rev. A **76**, 022510 (2007).
[19] F. Scazza, C. Hofrichter, M. Höfer, P. C. De Groot, I. Bloch, and S. Fölling, Nat. Phys. **10**, 779 (2014); **11**, 514 (2015).
[20] G. Cappellini, M. Mancini, G. Pagano, P. Lombardi, L. Livi, M. Siciliani de Cumis, P. Cancio, M. Pizzocaro, D. Calonico, F. Levi, C. Sias, J. Catani, M. Inguscio, and L. Fallani, Phys. Rev. Lett. **113**, 120402 (2014); **114**, 239903(E) (2015).
[21] M. Olshanii, Phys. Rev. Lett. **81**, 938 (1998).
[22] S. Fölling (private communication).
[23] The density of state (DoS) diverges in the zero-energy limit for an infinitely large one-dimensional system. In the realistic system with finite size, although the DoS does not diverge, it still significantly increases when the energy decreases. Thus the low-energy states also contribute most to the scattering problem. In addition, in the experiments the size of the system is much larger than the characteristic length of the longitudinal trapping potential of the $|e\rangle$ atom. As a result, the infinitely-large-size approximation is applicable.
[24] P. Massignan and Y. Castin, Phys. Rev. A **74**, 013616 (2006).
[25] Y. Nishida and S. Tan, Phys. Rev. Lett. **101**, 170401 (2008).
[26] S. Tan, Phys. Rev. Lett. **109**, 020401 (2012).
[27] D. Suchet, Z. Wu, F. Chevy, and G. M. Bruun, Phys. Rev. A **95**, 043643 (2017).
[28] G. Lamporesi, J. Catani, G. Barontini, Y. Nishida, and M. Inguscio, and F. Minardi, Phys. Rev. Lett. **104**, 153202 (2010).
[29] L. Riegger, N. D. Oppong, M. Höfer, D. R. Fernandes, I. Bloch, and S. Fölling, arXiv:1708.03810.